

How Predictable is the Northern Hemisphere Summer Upper-Tropospheric Circulation?

June-Yi Lee, Bin Wang and Q. Ding

IPRC and Atmospheric Department, University of Hawaii, USA

K.-J. Ha *Pusan National University, Korea*

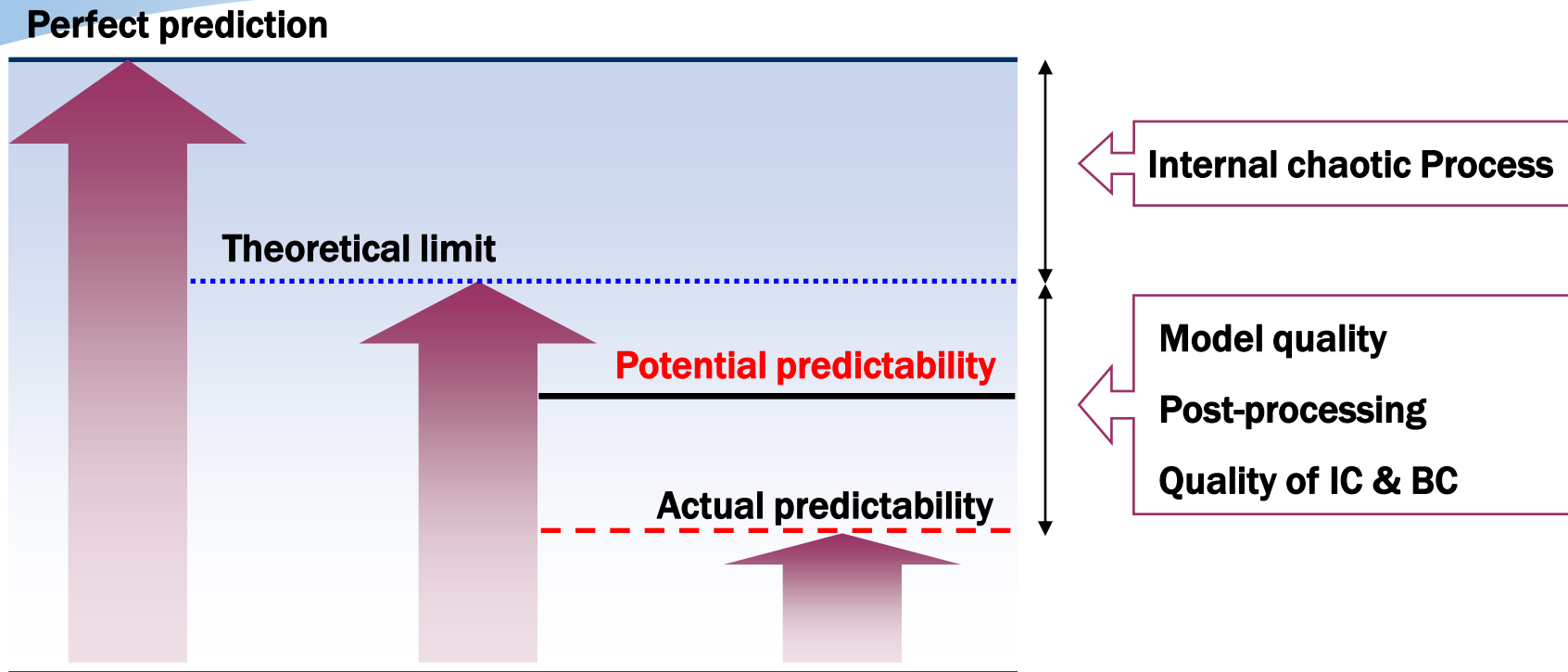
A. Kumar *NCEP/CPC, USA*

B. Stern *NOAA/GFDL, Princeton University, USA*

O. Alves *CAWCR, Bureau of Meteorology, Australia*



Seasonal Climate Predictability



From Prof. In-Sik Kang's Lecture, Monsoon Institute, Feb 2008

Predictability limits for seasonal climate variability depend on the fraction of signal and noise variability. **From the observed data alone, separation of the total seasonal variance into its signal and noise components remains difficult and controversial issue.**

Ensemble simulations of a stand-alone atmospheric model have been used to estimate signal-to-noise ratio of seasonal climate variability.

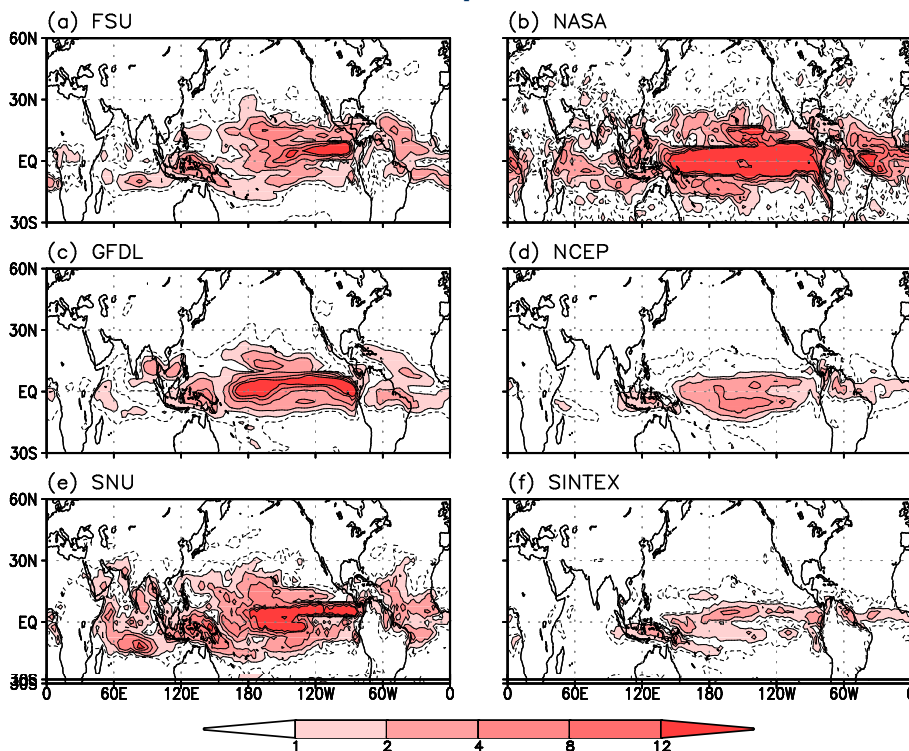


Seasonal Climate Predictability

✓ How to determine the **fractional signal variance (the predictable part of total variance)** and **predictability** of seasonal climate anomalies remains an unresolved issue.

✓ The conventional **signal-to-noise ratio approach is highly model-dependent** (Charney and Shukla 1981; Shukla 1998; Rowell et al. 1998; Kang and Shukla 2006 and many others).

Signal-to-noise ratio JJA Precipitation



✓ **Total Var = Signal Var (σ_{SST}^2) + Noise Var (σ_{INR}^2)**

$$\sigma_{SST}^2 = \sigma_{EN}^2 - \frac{1}{n} \sigma_{INR}^2 \quad \sigma_{EN}^2 = \frac{1}{N-1} \sum_{i=1}^N (x_i - \bar{x})^2$$

$$\bar{x} = 1/(Nn) \sum_{i=1}^N \sum_{j=1}^n x_{ij}$$

$$\sigma_{INR}^2 = \frac{1}{N(n-1)} \sum_{i=1}^N \sum_{j=1}^n (x_{ij} - \bar{x}_i)^2$$

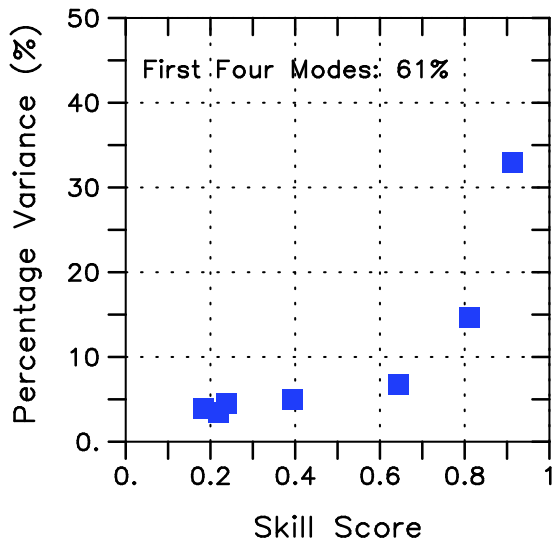
✓ **Signal-to-noise ratio**
= Signal Var / Noise Var



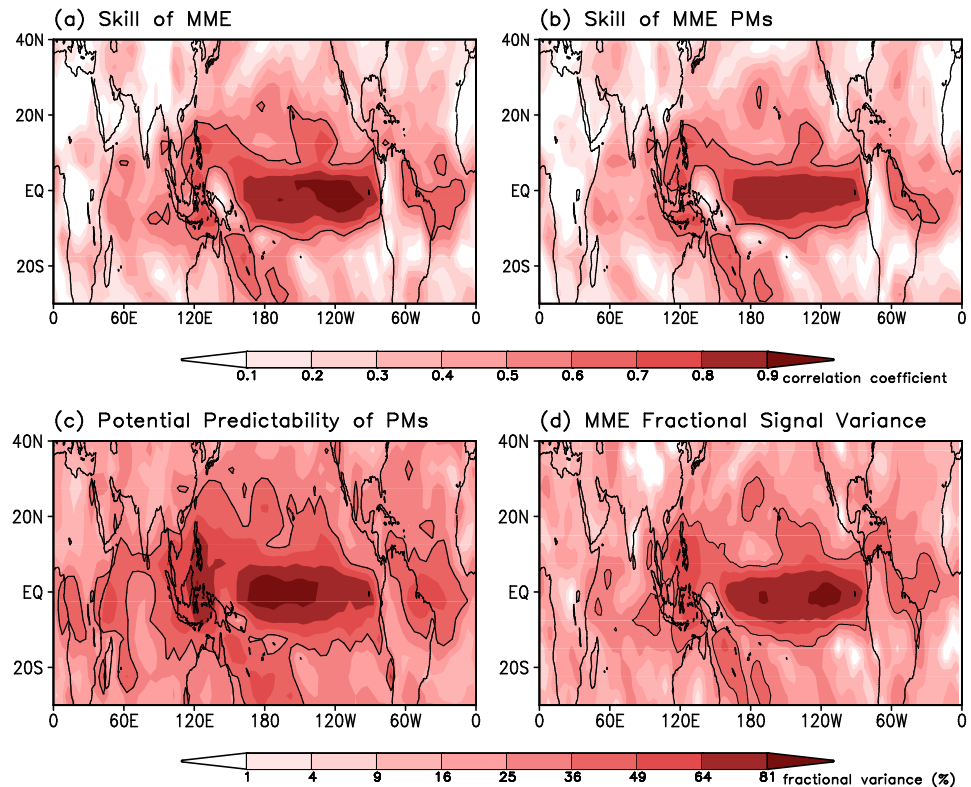
Predictable Mode Analysis

✓ We suggest a way to estimate seasonal climate predictability which relies on **identification of “predictable” leading modes of the observed interannual variation** using both observation and the state-of-the-art MME retrospective forecast. **The predictability is quantified by the fractional variance accounted for by these “predictable” leading modes.**

Identification of “predictable” leading modes from season-reliant EOF modes of seasonal precipitation over the global Tropics



Attained forecast skill and attainable predictability of Seasonal Precipitation over the global Tropics

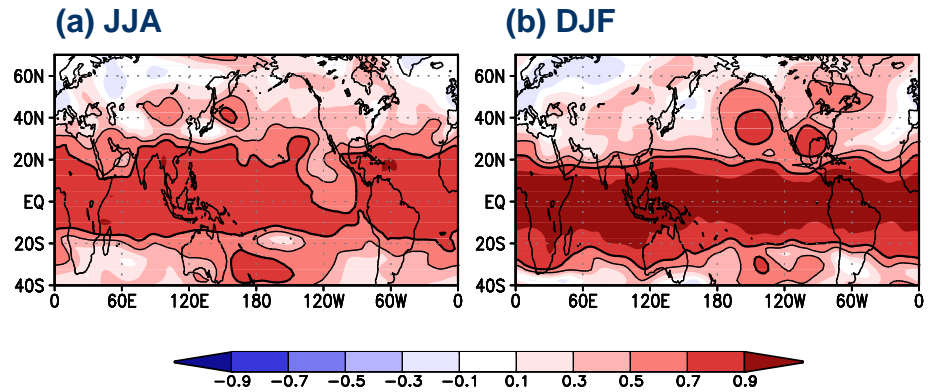




Background

✓ Using 14 climate prediction models, Wang et al. (2009) showed that the **MME prediction has useful forecast skill over some specific geographical locations** including East Asia and western North America, suggesting that **“predictable patterns” may exist in the NH extratropics during summer** and may be **associated with the tropical-extratropical teleconnection patterns.**

MME Temporal Correlation Skill for 500-hPa GPH



✓ In recent decades, **teleconnection patterns of boreal summer atmospheric circulation in the NH** from either a local or global point of view have received much attention, **mainly due to the Asian summer monsoon variability concurrent with either El Niño-Southern Oscillation (ENSO)** (Lau 1992; Kiapalani and Singh 1993; Kiapalani et al. 1997; Zhang 1999; Krishnan and Sugi 2001; Wang et al. 2001, 2003; Ding and Wang 2005; Hu et al. 2005; Liu et al. 2008; Ogasawara and Kawamura 2008) **or North Pacific SST variability** (Kawamura 1994; Park and Schubert 1997; Lau et al. 2000, 2003, 2004a and b; Lau and Weng 2000, 2002).

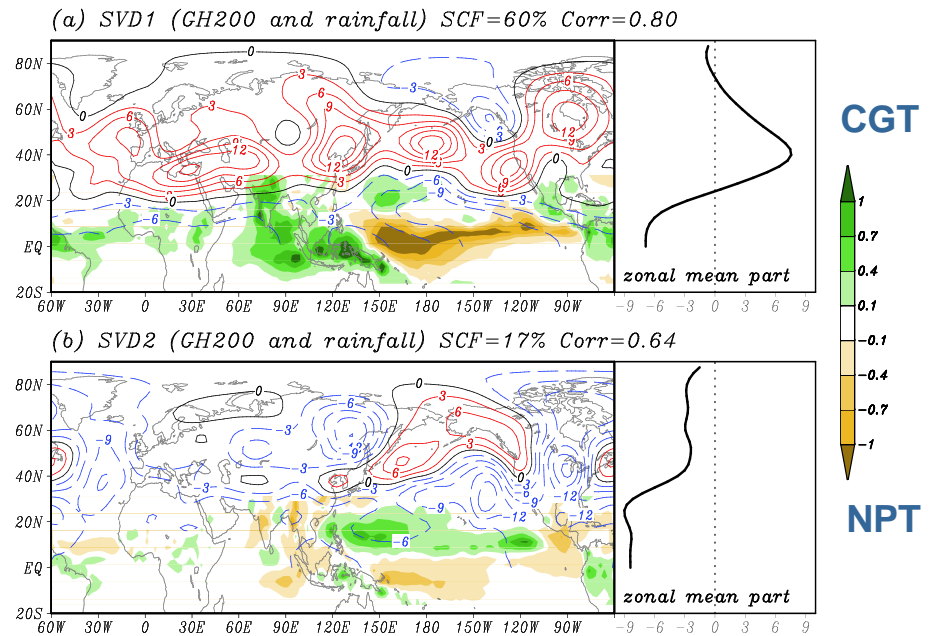


Background

✓ Ding and Wang (2005) demonstrated that on interannual time scales, **a circum global teleconnection (CGT) pattern exists during the NH summer which links regional teleconnection patterns with each other shown in previous findings such as the Indian summer monsoon (ISM)-East Asian summer monsoon (EASM) (Wang et al. 2001; Krishnan and Sugi 2001; Wu and Wang 2002) the silk road (Enomoto et al. 2003), and the Tokyo-Chicago express (Lau et al. 2004a) pattern.**

✓ In spite the fact that teleconnection patterns in boreal summer are weaker than its winter counterpart, the previous studies have demonstrated that they are **intimately coupled to surface temperature and precipitation variability in the NH extratropics and may act as source of climate variability and predictability over the region of interest.**

SVD analysis between GH200 and rainfall (JJAS, 1948-2005)





Data and Model Description

- ✓ **Attainable potential predictability of JJA 200-hPa GPH in the NH is estimated using observation (NCEP/DOE reanalysis II) and three coupled models' retrospective forecast for 25 years of 1981-2005.**
- ✓ **To identify dominant leading modes, EOF analysis is applied to JJA 200-hPa GPH in the NH.**

Description of models and their retrospective forecast

Coupled Models: NCEP CFS, GFDL CM2.1, BMRC POAMA

Period : 25 years of 1981 - 2005

Initial Condition: Jan 1, Feb 1, Mar 1, Apr 1, May 1, Jun 1

Target Season: JJA

Target Variables: Geopotential Height (GPH) at 200 hPa

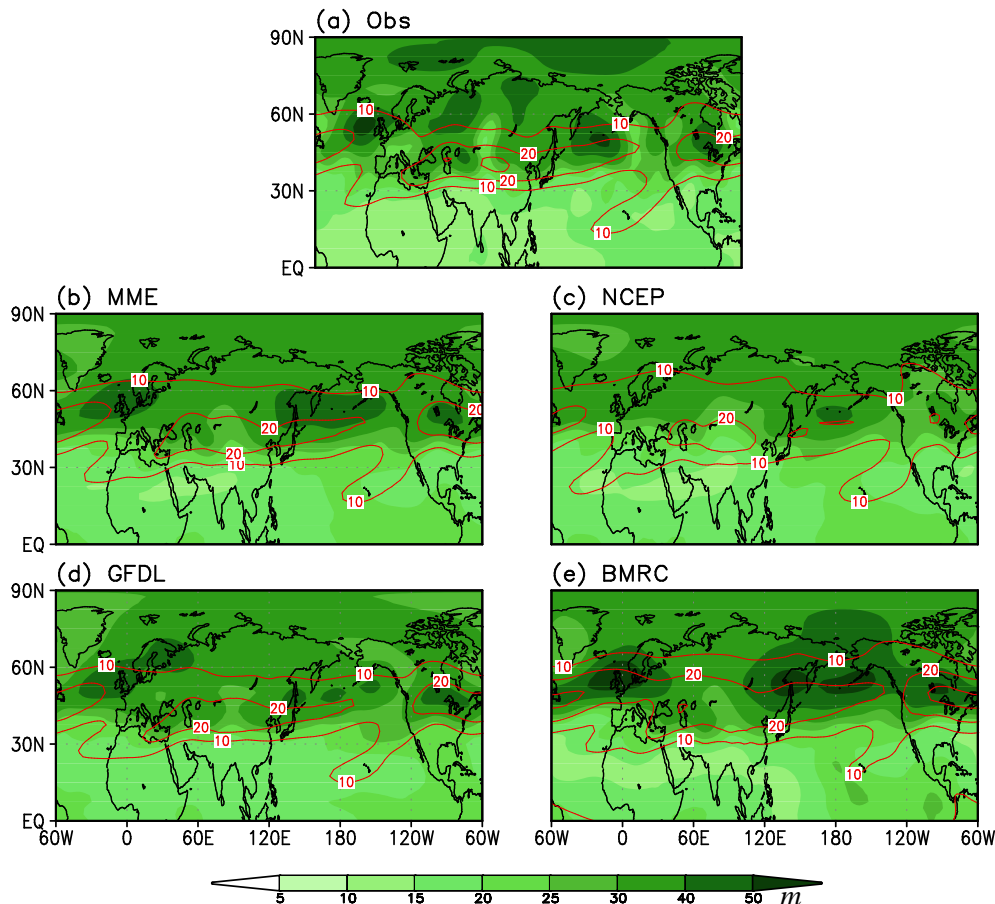
Institute (Model Name)	AGCM	OGCM	Ensemble Member	Period & forecast lead time	Reference
BMRC (POAMA1.5)	BAM 3.0d	ACOM2	10	1980-2006 9 months	Zhong et al. (2005)
	T47 L17	0.5-1.5°lat x2° lon L31			
GFDL (CM2.1)	AM2.1	OM3.1 (MOM4)	10	1979-2005 12 months	Delworth et al. (2006)
	2°latx2.5°lon L24	1/3° lat x 1° lon L50			
NCEP (CFS)	GFS T62 L64	MOM3 1/3° lat x 1° lon L40	15	1981-2008 9 months	Saha et al. (2006)



Evaluation of the Prediction of JJA Extratropical Climate

Couple models' capability in simulating mean state and variability of JJA atmospheric circulation

Climatology of U200 (red contour) and Standard Deviation of Z200 (shading)



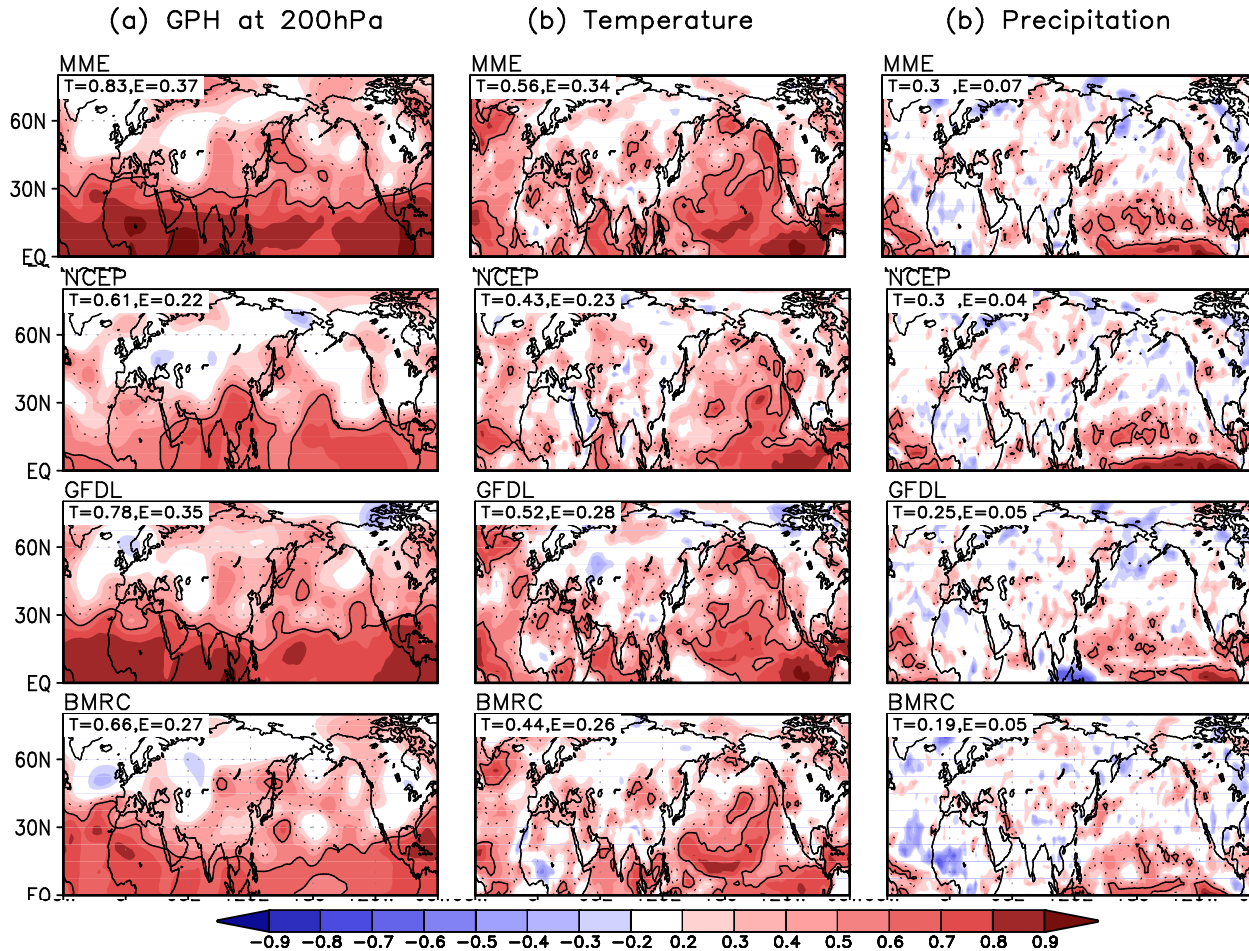
➤ The three coupled models and their MME capture, to some extent, the location of summertime jet streams, but have difficulty in capturing the observed variability centers except over the northeast Atlantic Ocean and northern North America.

➤ Differently from observation, the MME has strong variability over the northern part of East Asia.



Evaluation of the Prediction of JJA Extratropical Climate

Temporal Correlation Coefficient (TCC) Skill for One-month Lead JJA Prediction (May 1 initial condition)

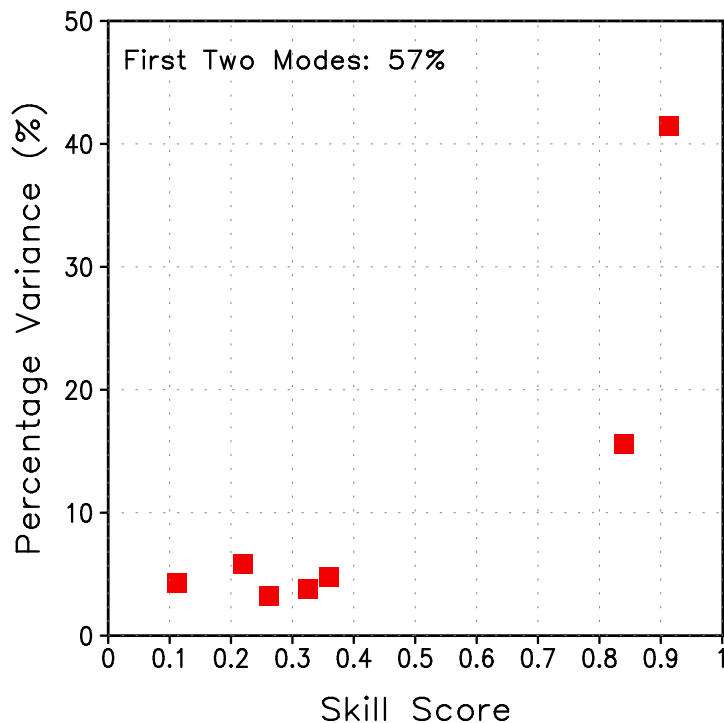


There are specific locations in which all coupled models tend to have significant forecast skills. It is of importance to understand the source of those prediction skills in the current coupled model and identify predictable modes of climate variability.



Identification of Predictable Modes: How Many Modes Are Predictable?

Scatter Diagram of
skill score and percentage variance for each EOF mode



Two basic criteria for determining predictable Modes

- 1. In observation, predictable mode should explain large parts of the total variability and be statistically separated from other higher (or unpredictable) modes.**
- 2. The state-of-the-art climate prediction models should be capable of predicting these major modes.**

Skill Score: $\text{SQRT}(\text{PCC} \cdot \text{TCC})$

TCC: Temporal correlation skill for PC time series for each mode

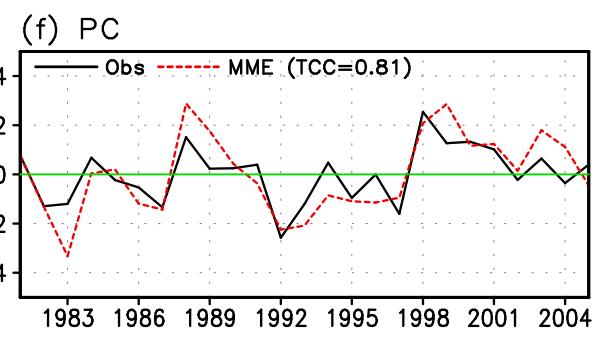
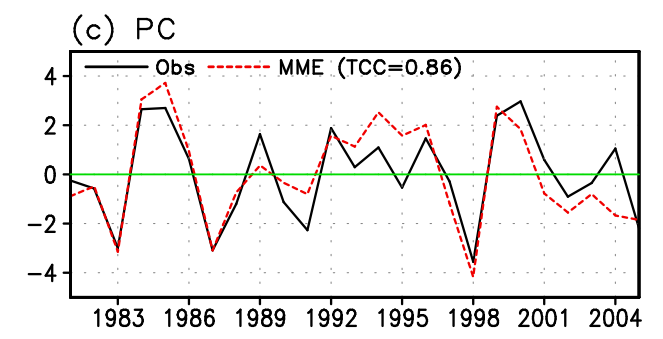
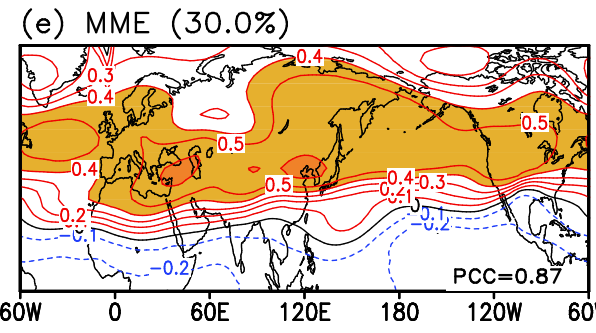
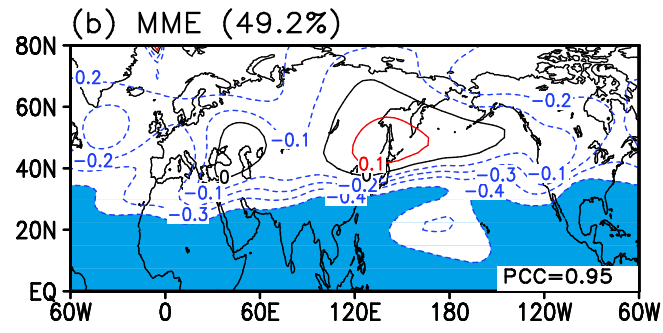
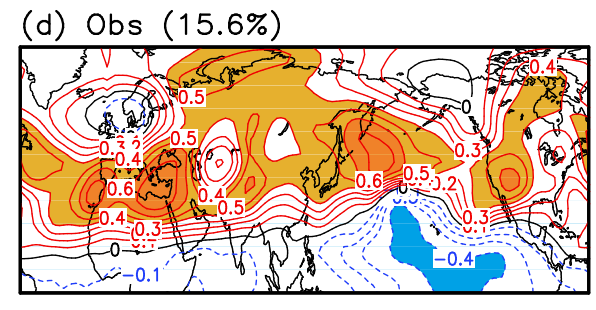
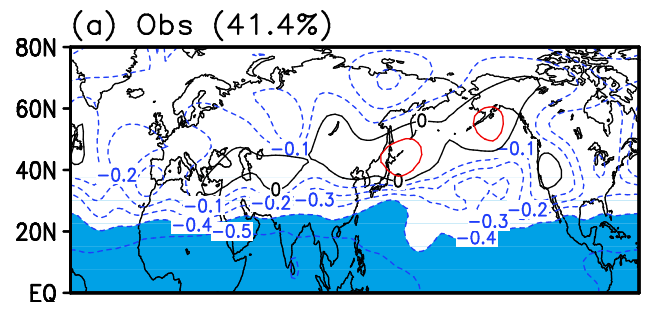
PCC: Pattern correlation skill for eigen vector for each mode



Characteristics of the Predictable Modes

EOF1

EOF2





Decomposition of total field into the predictable and unpredictable part

Area-averaged Fractional Variance for Each EOF Mode

	EOF1		EOF2	
	Tropics	Extra tropics	Tropics	Extra tropics
Obs	76.8%	13.4%	7.2%	22.0%
MME	81.1%	25.4%	9.0%	45.1%

In observation, **the first mode** accounts for 76.8% (13.4%) of total variance over the Tropics (Extratropics) in observation and thus **represents the tropical atmospheric variability**, while **the second mode loads more variability over the Extratropics** accounting for 22.0% of total variance

Decomposition of total field (Z200) into the predictable (Z200_{pred}) and unpredictable (Z200_{unpred}) part

$$Z200_{pred}(lon, lat, t) = \sum_{i=1}^{N_p} \lambda_i EV_i(lon, lat) PC_i(t)$$

$$Z200_{unpred}(lon, lat, t) = \sum_{i=N_p+1}^{N_T} \lambda_i EV_i(lon, lat) PC_i(t)$$

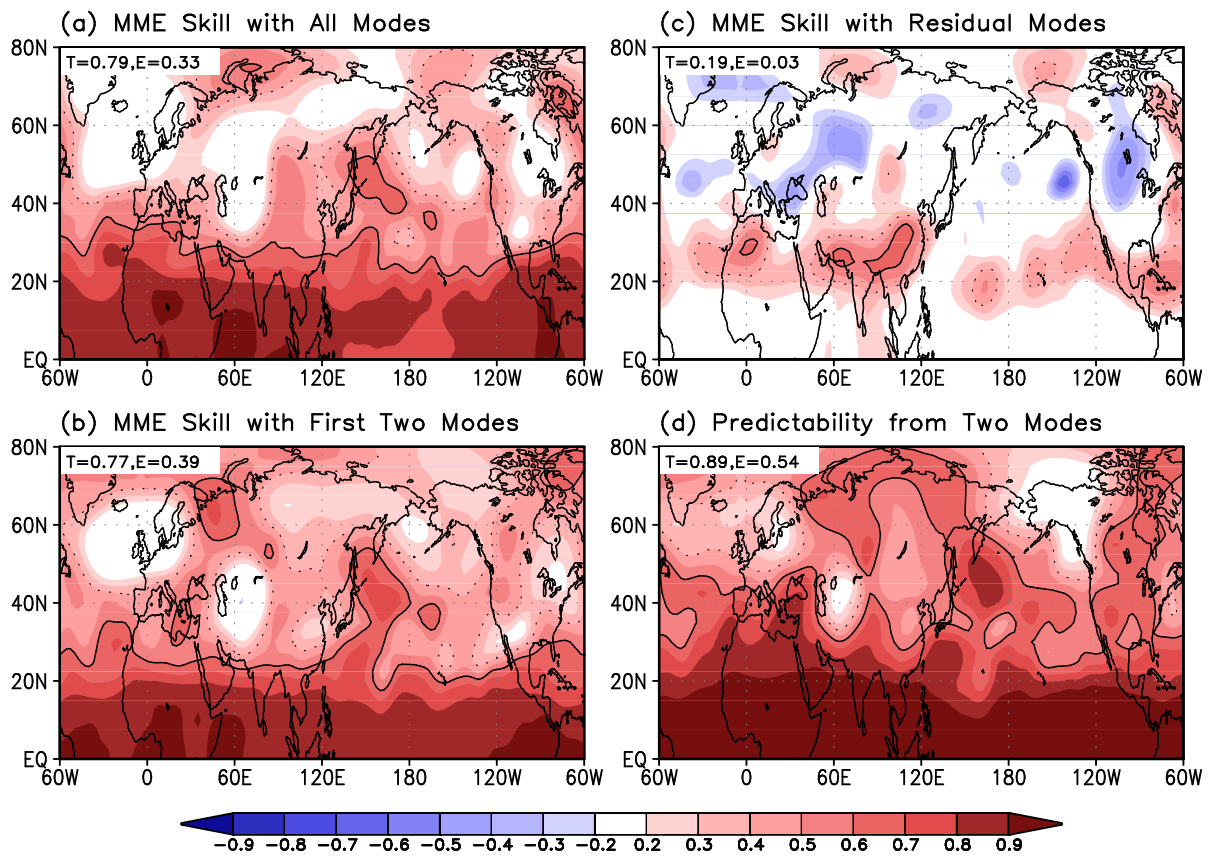
N_p : The total number of predictable modes
 N_T : The total number of EOF modes

From the conventional point of view, potential predictability can be defined by the fractional variance of the predictable part. In this case, about **84% (35.4%)** of total variability is potentially predictable over **the NH Tropics (Extratropics)**.

In this study, however, **the realizable potential predictability is estimated by the TCC between the observed total field and the observed predictable part** in order to facilitate comparison with the MME prediction skill. Thus, **it represents the achievable forecast skill if climate prediction models can perfectly predict the observed predictable modes.**



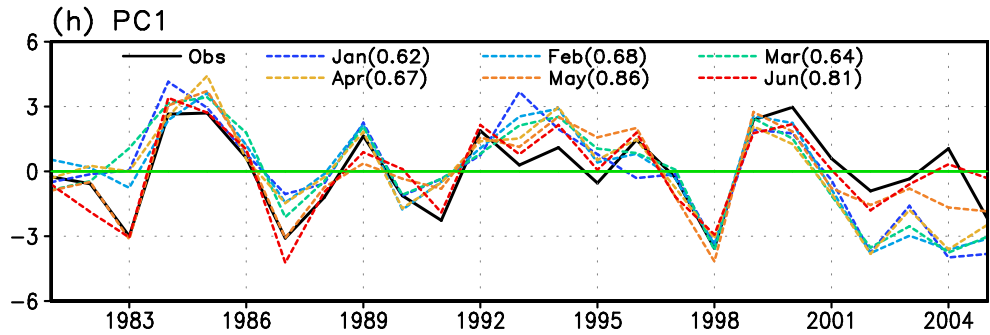
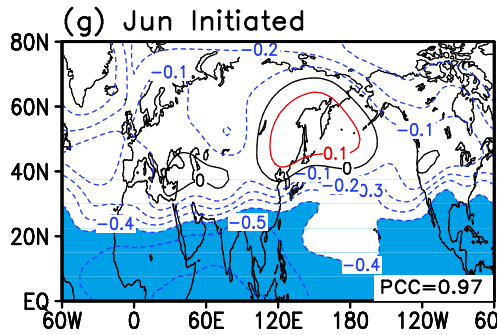
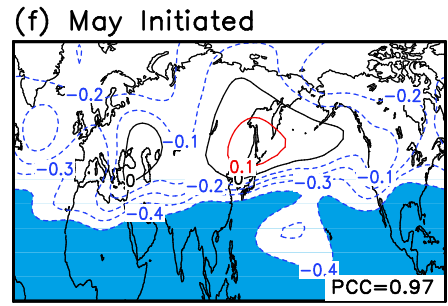
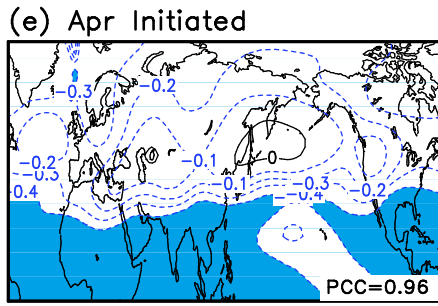
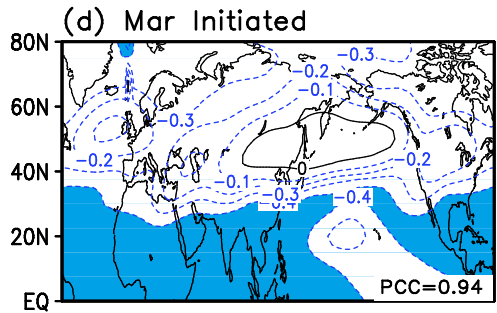
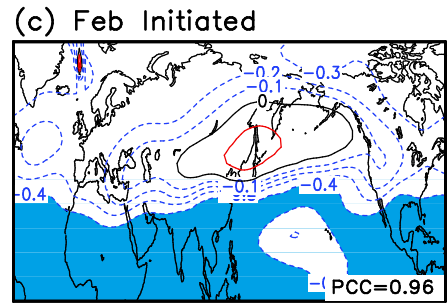
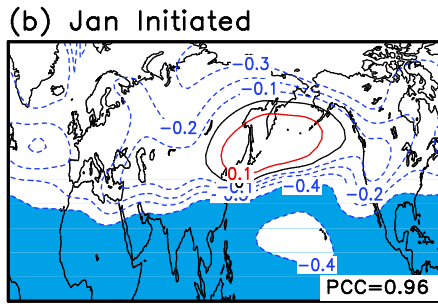
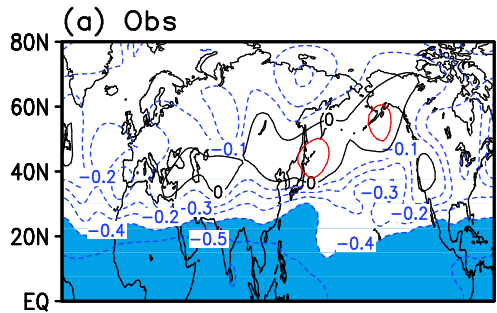
Achieved forecast skill and potential predictability



- ✓ The MME prediction skill for the JJA NH 200-hPa GPH basically comes from the coupled models' capability in predicting the first two EOF modes of variability. The residual higher modes cannot be captured by the MME.
- ✓ The one-month lead MME prediction skill is far below the achievable predictability over the extratropics. Nonetheless, the predictable part of the MME prediction better predicts the observed variability where the potential predictability is higher.

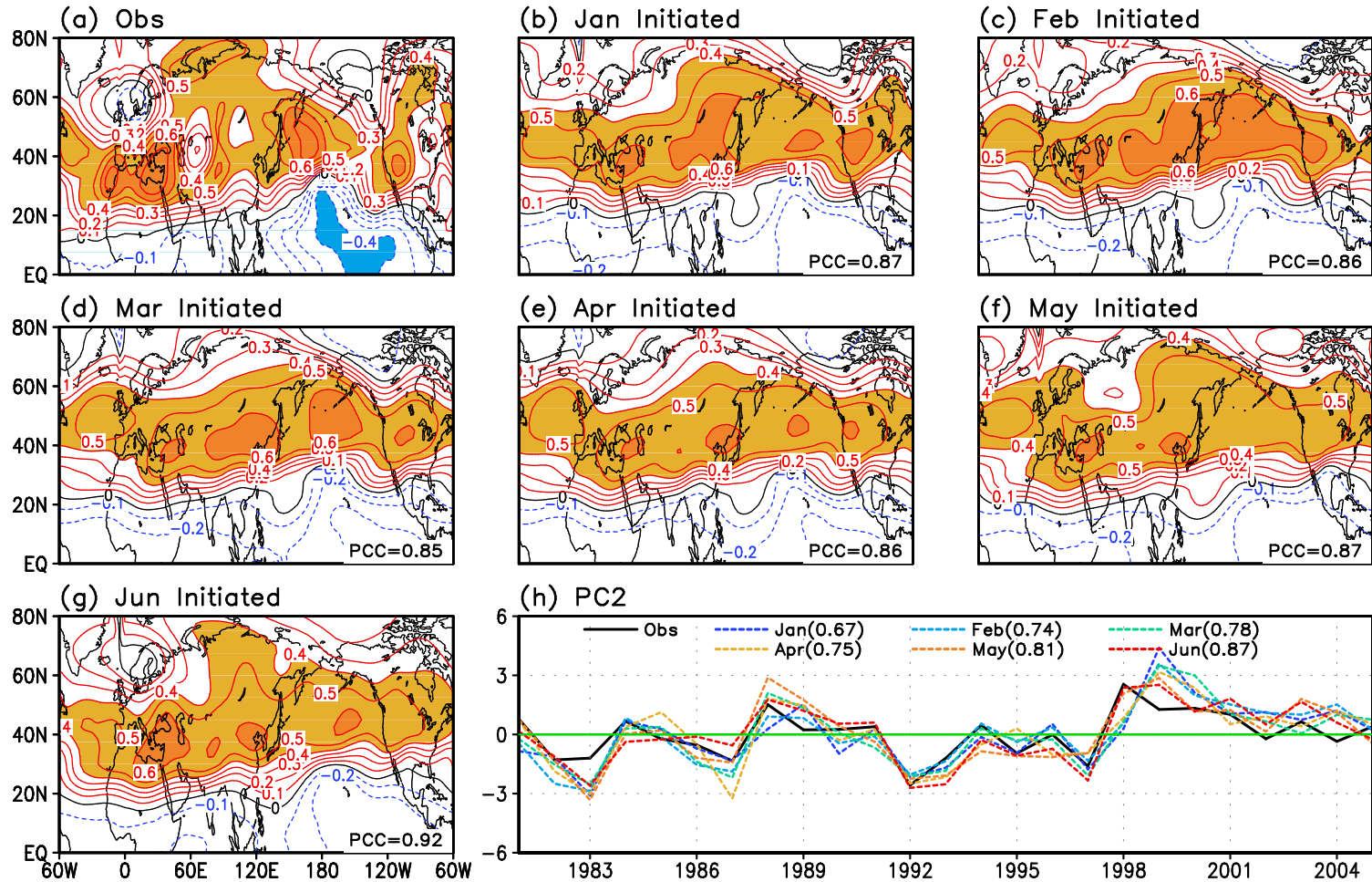


Impact of forecast lead time: EOF1





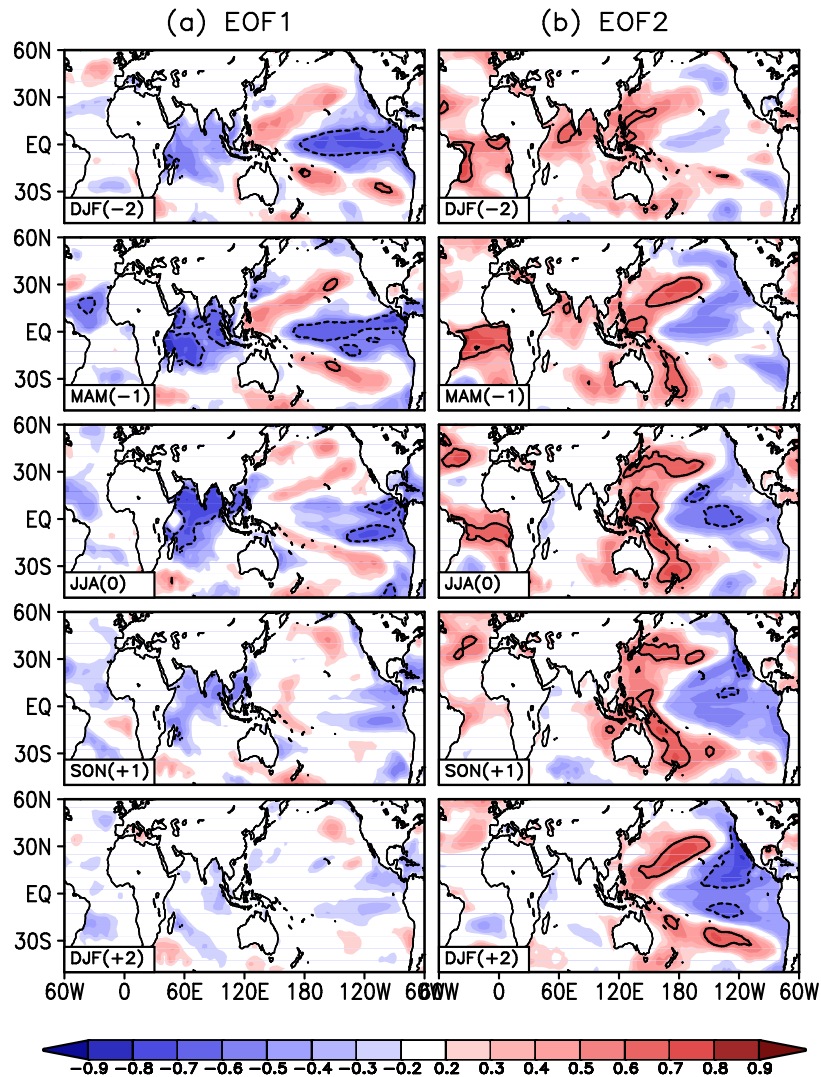
Impact of forecast lead time: EOF2





Source of predictability: SST-PC Relationship

Temporal Correlation for Seasonal SST Against PCs



✓The long-lead predictability of the EOF1 comes mainly from **the prolonged impacts of ENSO** as the EOF1 tends to occur during the summers after the mature phase of the ENSO.

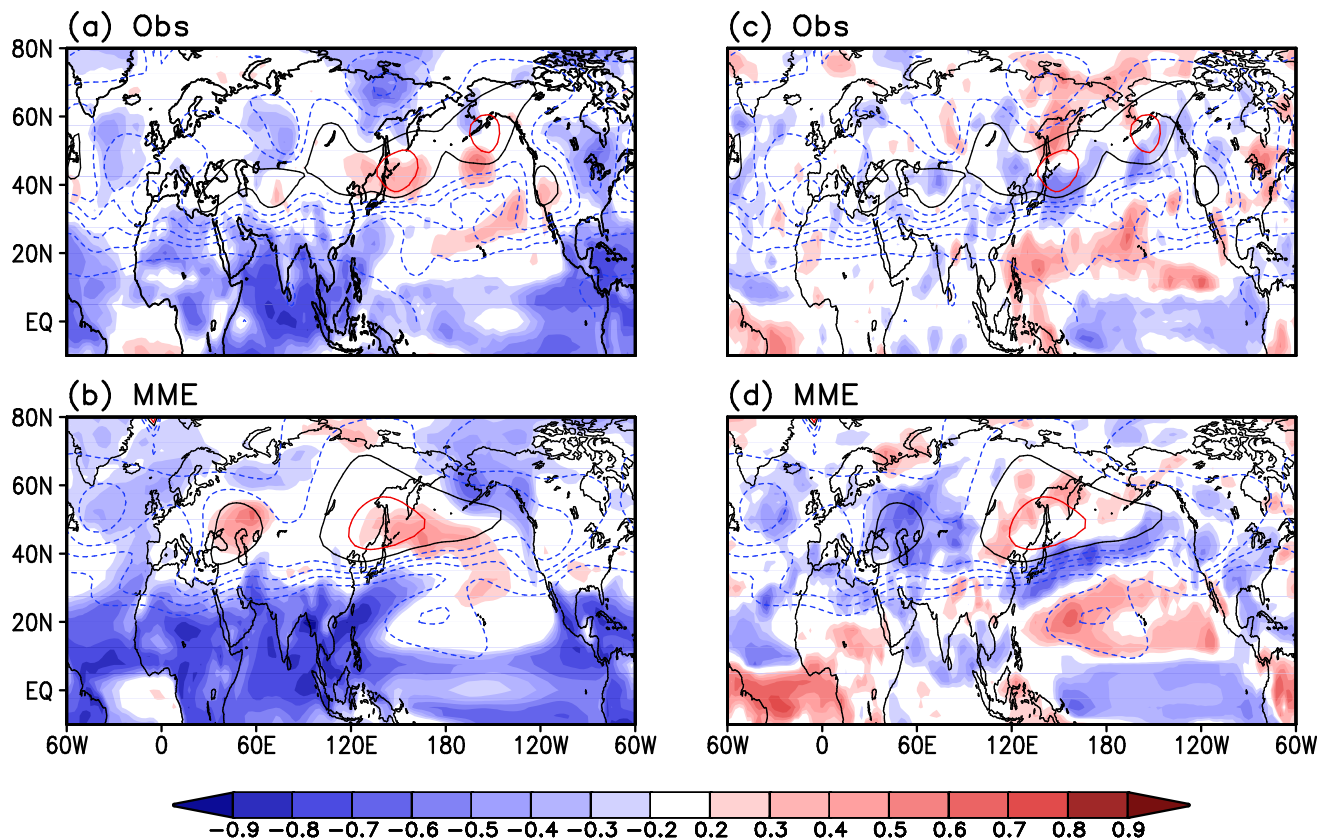
✓The second EOF (EOF2) mode is related to **the developing ENSO** on interannual time scale and also **the SST variability over the North Pacific and Atlantic Ocean** on interdecadal time scale.



Climate Anomalies Associated with PC1

Temperature

Precipitation



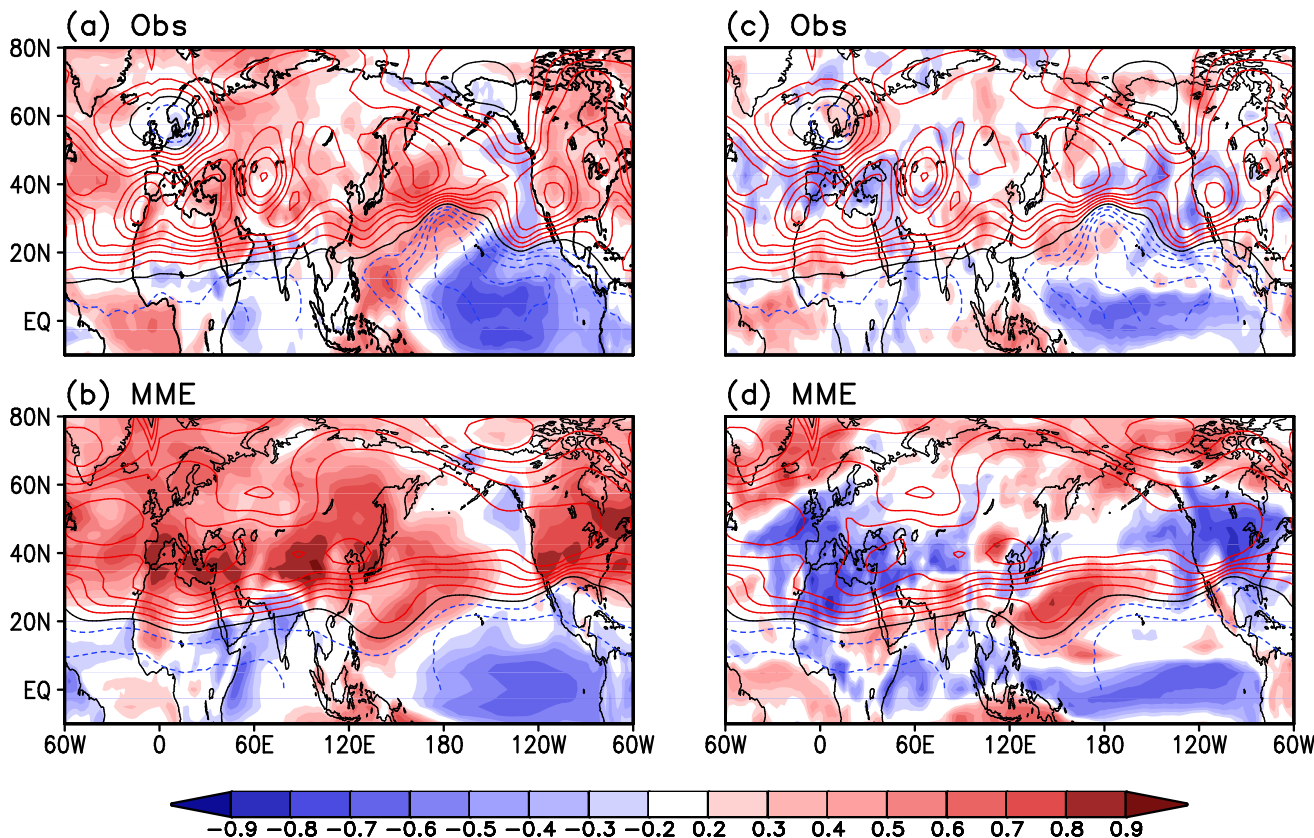
In both observation and the MME prediction, the first two leading modes are accompanied by significant rainfall and surface air temperature anomalies in the continental region of the Extratropics. The MME's success in predicting the first EOF mode likely leads to better prediction of JJA precipitation anomalies over East Asia one-month ahead.



Climate Anomalies Associated with PC2

Temperature

Precipitation

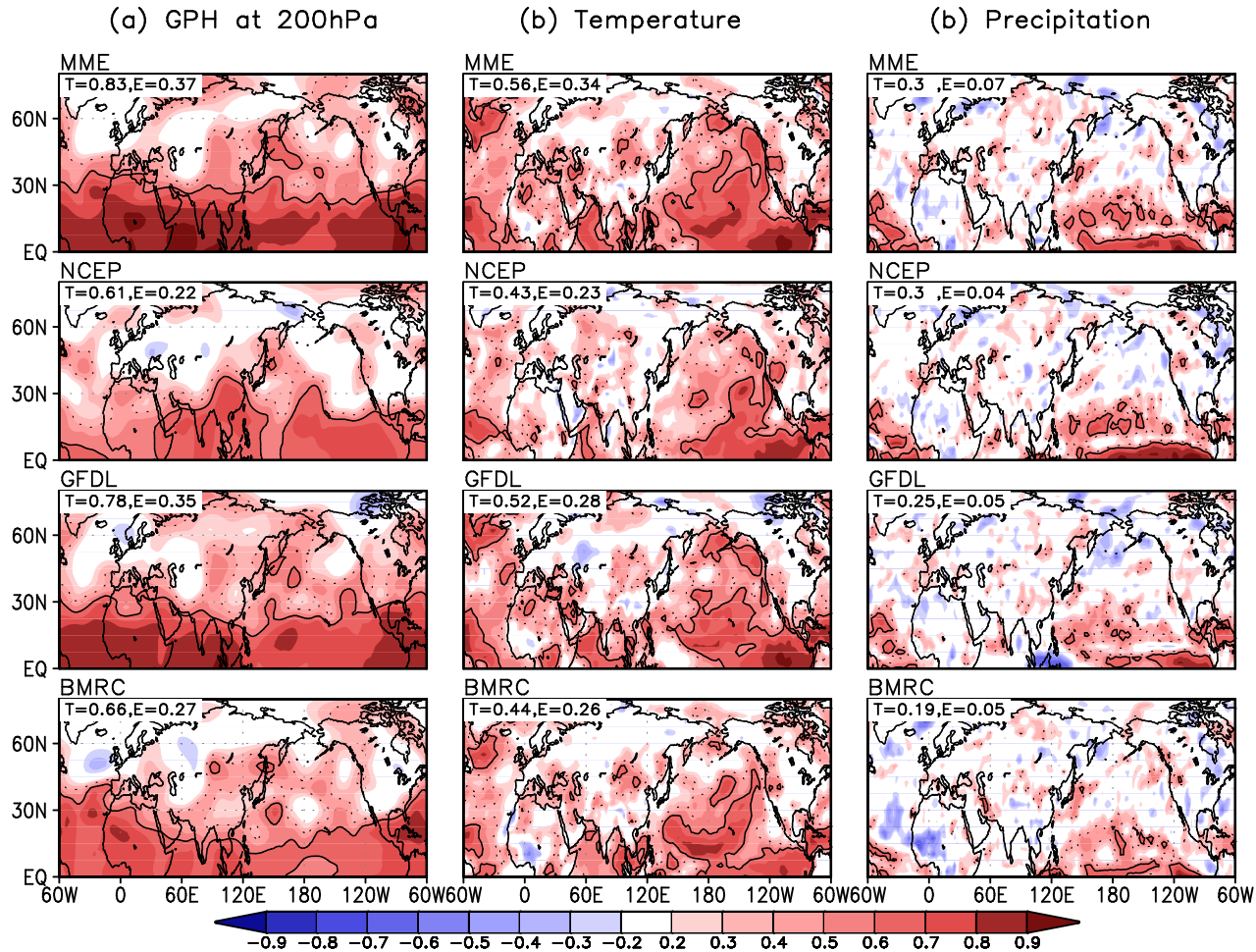


The MME's success in predicting the second EOF mode likely leads to better prediction of JJA precipitation anomalies over Central and Southern Europe one-month ahead.



Evaluation of the Prediction of JJA Extratropical Climate

Temporal Correlation Coefficient (TCC) Skill for One-month Lead JJA Prediction (May 1 initial condition)



There are specific locations in which all coupled models tend to have significant forecast skills. It is of importance to understand the source of those prediction skills in the current coupled model and identify predictable modes of climate variability.



Summary

1

The first two leading empirical orthogonal function (EOF) modes of summertime upper-tropospheric circulation in the Northern Hemisphere (NH) are identified as **predictable modes** using the NCEP-NCAR reanalysis data and three coupled models' hindcast data from NCEP, GFDL, and BMRC for 25 years of 1981-2005 for a number of reasons. First, **these observed modes are statistically well separated from the higher modes** and account for the large fraction of total variability. Second, these modes have clear physical interpretations and **their sources are understood in terms of ENSO teleconnection dynamics**. Third, **the current MME is capable of predicting the spatial structure and temporal variation of these modes** with a high fidelity even at a five-month lead.

Three coupled models and their multi-model ensemble (MME) prediction skills for JJA 200-hPa geopotential height (GPH) in NH basically come from **the coupled model's capability in predicting the first two modes of interannual variability**.

2

In observation (the one-month lead MME prediction), the first two EOF modes account for 84 % (90.1%) and 35.4 % (70.5%) of the total variance over the Tropics and the Extratropics, respectively, in NH, indicating that the MME highly overestimates fractional variance of the first two modes particularly over the Extratropics.



Summary

3

The long-lead predictability of **the first EOF mode** comes mainly from El Niño-Southern Oscillation (ENSO) since **it tends to occur summers after mature phase of ENSO**. The MME well predicts both temporal and spatial characteristics of the first mode even at 5-month lead (January initial condition) with a temporal correlation coefficient (TCC) skill for principal component (PC) of 0.62 and a pattern correlation coefficient (PCC) skill for eigenvector of 0.96.

4

The second EOF mode is related with not only **developing ENSO on interannual time scale** but also **SST variability over the North Pacific and Atlantic Ocean on interdecadal time scale**. The MME is also capable of capturing the second mode even at 5-month lead with a TCC skill of 0.67 and a PCC skill of 0.87. While the MME well predicts the zonally symmetric part of the second eigenvector, it has difficulty to capture prominent wavelike structure of it, so call circumglobal teleconnection (CGT) pattern. Each coupled model has a significantly different CGT pattern from each other as well as from the observed counterpart.

5

In both observation and MME prediction, the first two leading modes are accompanied by significant rainfall and surface air temperature anomalies in the continental region of the Extratropics. **The MME's success in predicting the EOF1 (EOF2) is likely to lead to a better prediction of JJA precipitation anomalies over East Asia and the North Pacific (Europe and western North America) one month ahead.**